Laser induced fluorescence observations of a multipolar argon discharge

Gérard Bachet, Laurence Chérigier-Kovacic, M. Carrère, Fabrice Doveil

Laserinduced fluorescence observations of a multipolar argon discharge

G. Bachet, L. Chérigier, M. Carrère, and F. Doveil

Citation: Physics of Fluids B: Plasma Physics (1989-1993) **5**, 3097 (1993); doi: 10.1063/1.860642
View online: http://dx.doi.org/10.1063/1.860642
View Table of Contents: http://scitation.aip.org/content/aip/journal/pofb/5/8?ver=pdfcov
Published by the AIP Publishing

Laser-induced fluorescence observations of a multipolar argon discharge

G. Bachet, L. Chérigier, M. Carrère, and F. Doveil
Equipe Turbulence Plasma de l'URA 773 du CNRS et de l'Université de Provence, Institut Méditerranéen de Technologie, F13451 Marseille Cedex 13, France

(Received 4 January 1993; accepted 4 May 1993)

Observations carried out with a laser-induced fluorescence diagnostic on several configurations of a multipolar discharge are presented. This diagnostic allows very accurate measurements of the ion velocity distribution function in the argon plasma and reveals the presence of double-hump velocity distribution functions due to ion acceleration in the static plasma potential and ion reflection on a multipolar magnetic field. These observations give a new insight to ion temperature and ion drifts inside the device.

I. INTRODUCTION

Laser-induced fluorescence[1,2] is a nonintrusive technique, based on the Doppler effect,[3] which allows a very accurate measurement of the velocity profile of the ion distribution function in a plasma. This diagnostic has been widely used for studying magnetized plasmas,[4,5] but only a few experiments[6] have been reported concerning low-density unmagnetized plasmas like those obtained in multipolar discharges.[7] These devices have played an important role in the study of fundamental plasma phenomena such as wave[8,9] or soliton[10] propagation; more recently, they have been used a great deal in the plasma processing industry.[11]

However, the behavior of the steady-state plasma created in such a device by a thermoelectronic discharge in argon is far from being completely understood. For example, in the collisionless plasmas at low gas pressure, the importance of charged particle acceleration in the static electric field of the plasma sheath, and trapping or reflection by the multipolar magnetic field, remains to be explored.[12,13]

In order to investigate such phenomena, we have developed a laser-induced fluorescence diagnostic in a multipolar device, specially designed to allow both longitudinal and radial exploration of the plasma.

Ion flow measurements have already been made with probes in a large-volume stationary plasma.[14] The optical technique allowed us to carefully study the ion motion in our multipolar device. Beside showing the sharp resolution obtained on the measurement of the ion velocity distribution function, this paper mainly concentrates on the role of the multipolar magnetic field in ion reflection and of plasma density gradients in the ion drift. The paper has been organized as follows. In Sec. II we review the principle of the laser-induced fluorescence diagnostic. In Sec. III we describe the experimental apparatus. In Sec. IV we present our results and in Sec. V we state our conclusions.

II. DIAGNOSTIC PRINCIPLE

The laser-induced fluorescence diagnostic is based on the Doppler effect. By scanning the cw beam of a single-frequency dye laser across the line corresponding to the transition $3d^2G_{9/2} \rightarrow 4p^2F_{7/2}$ of Ar^{II} at 611.492 nm, every velocity class of ions in the metastable level ($3d^2G_{9/2}$) can be explored. As sketched in Fig. 1(a), the upper level decays toward the lower one with a fluorescent emission at 460.957 nm. In fact, the intensity of the fluorescence is proportional to the number of metastable ions in the velocity distribution function whose velocity component $\mathbf{v}_{\text{laser}}$ in the direction of the laser beam satisfies the relation

$$\omega_{12} = \omega_{\text{laser}} - \mathbf{k}_{\text{laser}} \cdot \mathbf{v}. \tag{1}$$

In this relation, ω_{laser} and $\mathbf{k}_{\text{laser}}$, respectively, represent the scanning laser frequency and the wave number, and ω_{12} is the frequency of the above-mentioned transition. This relation defines the locality in ion velocity space $\mathbf{v}$. As is also sketched in Fig. 1(a), locality in space $\mathbf{r}$ is obtained by collecting the fluorescence at 90° to the incident laser beam. Thus the diagnostic allows to accurately probe the total ion phase space $(\mathbf{r},\mathbf{v})$.

III. EXPERIMENTAL SETUP

Figure 1(b) gives a sketch of the multipolar device. It is made of a cylindrical stainless steel vacuum vessel 45 cm in diameter and 80 cm long surrounded on the outside by 14 rows of permanent magnets with alternate polarizations. Inside the vessel, four lines of permanent magnets can be held in place on each of the two thick plane doors closing the ends of the cylinder. Accurate measurements of the static magnetic field have shown that it does not extend beyond 10 cm from the inner wall.

A turbomolecular pump is used to evacuate the device at a pressure in the range of 10^{-8} Torr. A Pirani gauge and an ionization gauge measure the base vacuum. A mass spectrometer gives the composition of the residual gases in the vessel. Once a good base vacuum is obtained, the argon gas is introduced in the vessel through a controlled microleak at a working pressure on the order of 10^{-4} Torr.

The plasma is created by a thermoelectronic discharge using three filament holders. One short filament holder merely consists of two conducting rods, which are insulated from the plasma by ceramics and between which a 2 cm long tungsten filament is stretched. Since the rods do not extend beyond 5 cm from the inner vessel wall and the short filament holder is located at an equal distance from the end doors, between two adjacent rows of permanent magnets, it can be inferred that the filament lies inside the

 0899-8221/93/5(8)/3097/6/$6.00

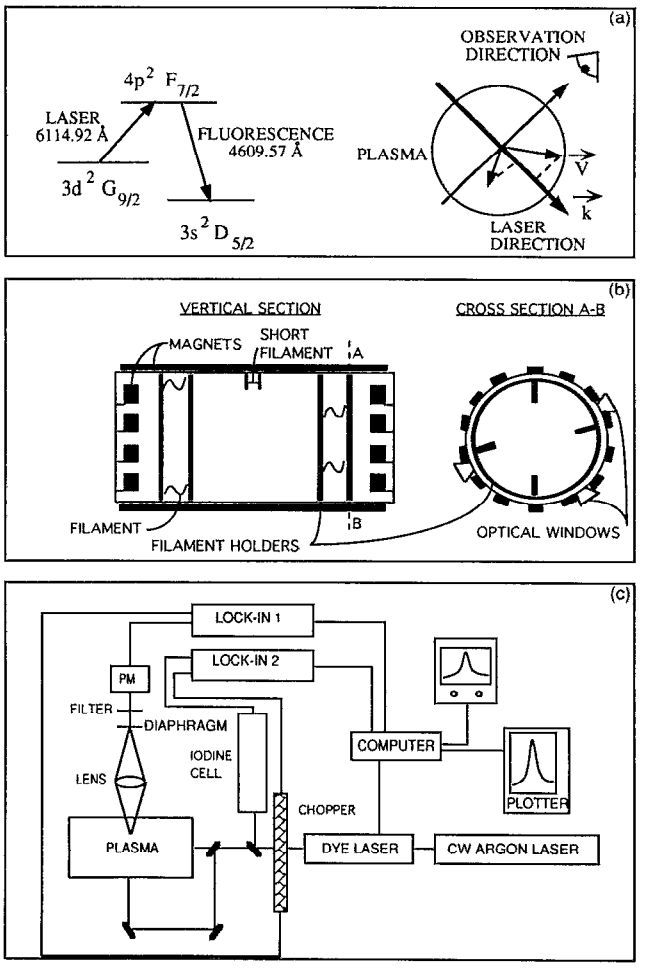

FIG. 1. (a) Energy level diagram. The distribution of the velocity component in the direction of the laser beam is measured. (b) Multipolar device: filament holders and magnets held by the doors are removable. (c) Schematic diagram of the experimental arrangement.

multipolar magnetic field. Each of the two other filament holders are composed of two 40 cm diam copper rings spaced 7 cm apart, insulated by ceramics, between which four tungsten filaments are stretched. For holder No. 1, the filaments are near the inner wall inside the multipolar magnetic field. For holder No. 2, the filaments are within the plasma in a region of a zero magnetic field. We will see later that each of these geometric configurations are important. Typically, a plasma is obtained with a 1 A discharge current, 50 V dc discharge voltage between the grounded wall of the vessel and one end of a filament holder and a working pressure in the range 10^{-4}–10^{-3} Torr. These working conditions give a partially ionized plasma having a charged particle density in the range 10^8–10^9 cm^{-3}. The ion mean-free path is in the range 70–10 cm.

Several Langmuir probes measure such parameters as the electronic density and temperature, the plasma potential, and the floating potential. One of these probes can be moved longitudinally to measure the axial plasma density profile, it can also be rotated to explore a slice of plasma. Two other probes can analyze the plasma transversally.

The main peculiarity of this multipolar device is the presence of three rectangular optical windows that extend in between two adjacent rows of permanent magnets along the generatrix of the cylinder. Two diametrically opposite windows allow the laser to be beamed transversally through the plasma from almost any position along the generatrix of the cylinder. The fluorescence is collected outside the device at about 90° to the incident beam through the third window. As shown by Eq. (1), the ion radial velocity distribution function can thus be measured at any position along the axis of the cylinder.

The incident laser beam can also be propagated longitudinally along the axis of the cylinder by means of two small portholes located on each of the plane end doors. By collecting the fluorescence through the same window as before, the ion axial velocity distribution function can thus also be measured at any position along the axis of the cylinder.

The laser-induced fluorescence diagnostic is displayed in the diagram in Fig. 1(c). It uses a cw 899-21 tunable ring dye laser from Coherent pumped by an Innova 306 argon ion laser. By moving a plane mirror attached to a slide, the laser beam can be very easily propagated longitudinally or transversally through the plasma. The laser beam is chopped and a lock-in amplifier is used to discriminate the fluorescent signal from the spontaneous emission of the plasma at the same frequency. A narrow bandpass interferential optical filter (1 nm) is used to eliminate unwanted radiation. An $f/2$ lens collects the fluorescence and forms the laser beam image, with a magnification of 0.6, on a 1 mm diam diaphragm, which then sets the spatial resolution of the diagnostic at 6 mm^3. A small part of the laser output is sent through an iodine cell and the iodine absorption gives an absolute calibration of the laser emission.

The entire diagnostic is under the control of an on-line 386 microprocessor computer. The laser scan is monitored and at each step of the scanning process the data on the level of iodine absorption on one hand and that of the fluorescence on the other hand is stored to 12 bits of accuracy. This computer is also used for processing the data.

Although the laser line width is 0.5 MHz, which corresponds to a resolution in velocity of 0.3 m/sec, we have restricted, for convenience, the frequency acquisition sampling to reach a "practical" resolution of 30 m/sec. The zero velocity is given by the wavelength of the $3d^2G_{9/2} \rightarrow 4p^2F_{7/2}$ transition of Ar^{II} in vacuum.

IV. RESULTS

A. Local ionization and ion reflection

In this configuration, the multipolar device is used without magnets on the doors, and the plasma is created with the short filament holder located between two magnetic cusps at an equal distance from both ends of the device. The argon working pressure is equal to 2.3×10^{-3} Torr, the filament current is 12 A, and the discharge voltage and current are, respectively, 60 V and 1 A.

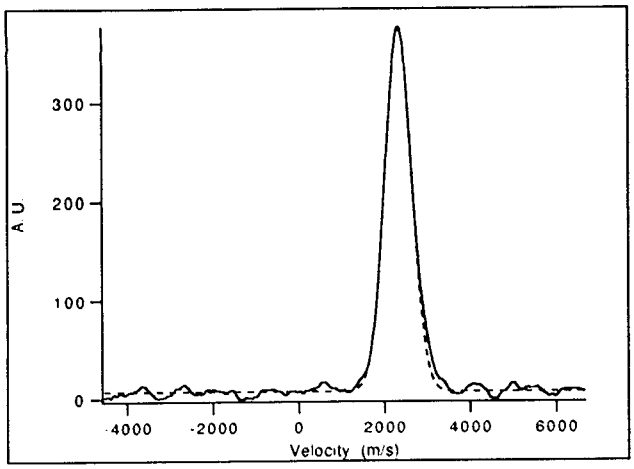

(a)

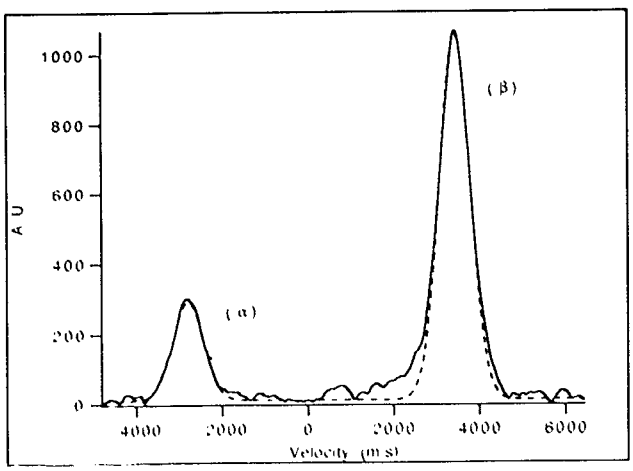

(b)

FIG. 2. (a) Longitudinal velocity distribution, presence of an ion drift. (b) Transversal velocity distribution, presence of drifting ions (β) reflected by the magnetic field (α).

The continuous line of Fig. 2(a) shows the longitudinal ion velocity distribution function measured along the axis at 9.5 cm from the center of the device. It clearly exhibits a longitudinal ion drift velocity component of 2.3 km/sec. We have verified that this shift depends on the point where the measurement is made. At the center of the device there is no shift: the distribution function is centered on zero. On one side of the filament holder, the mean velocity component is negative, and on the other side it is positive. The ion temperature is obtained by fitting a Maxwellian model to our data using the simplex method. The dashed curve of Fig. 2(a) corresponds to this type of fit and yields a longitudinal ion temperature of 0.04 eV to be compared to the 0.025 eV temperature of the neutral argon gas at room temperature. This result is consistent with previous measurements in a somewhat similar device.[6]

The transversal measurement for the same position in the device is shown by the continuous curve in Fig. 2(b). The transversal ion velocity distribution function exhibits two peaks corresponding to two ion drifts in opposite directions. The mean positive transversal velocity component is equal to 3.3 km/sec. The mean negative transversal velocity component is equal to −2.8 km/sec. The dashed curve of Fig. 2(b) is obtained by fitting a Maxwellian curve with the same temperature for both peaks, and gives a transversal temperature equal to 0.05 eV.

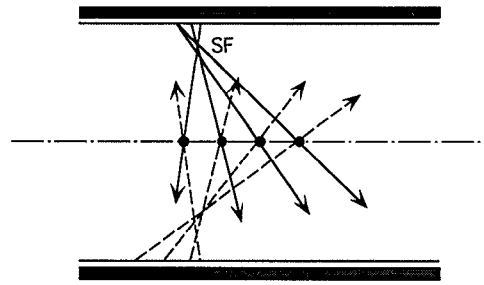

FIG. 3. Plot of the experimental velocity directions showing the localized ionization. Reflected ions are coming from an area located symmetrically to the source SF (short filament).

On Fig. 3, the velocity direction is plotted for each point, where both the longitudinal and the *positive* transversal components have been measured. This clearly shows that most of the ions are coming from a very small area located near the filament. The same plot can be made using the *negative* transversal velocity component. Surprisingly enough, it appears that the negative transversal component corresponds to ions coming from a point diametrically opposed to the localized source.

These measurements clearly show that, when using a filament located inside the multipolar magnetic field, the ionization remains localized around the filament. This has been verified by a numerical simulation, which computes the ion or electron trajectories in the multipolar magnetic field. Preliminary results have shown that primary electrons are trapped around the magnetic lines, and that not all the ions are lost to the wall. Some of them can be reflected by the magnetic field; this depends essentially on their incident velocity. The experimentally observed localization of reflected ions remains to be explained.

B. Wrong temperature evaluation due to overlapping distributions

Filament holder No. 2 is used with four filaments inside the plasma in a region outside the magnetic field. Magnet rows are added to the two end doors. The argon working pressure is equal to 1.0×10^{-3} Torr, and the discharge voltage and current are, respectively, equal to 50 V and 1 A.

Transversally, all along the device, we have observed that the ion distribution function remains centered on zero.

The continuous curve of Fig. 4(a) shows a measurement of the longitudinal ion velocity distribution at 15 cm from the center of the device, near the end door farther away from the filament holder. Two overlapping components of the distribution function can easily be defined. The larger one corresponds to ions drifting from the filament to the end door with a mean positive velocity equal to 0.45 km/sec, while the smaller one corresponds to ions drifting in the opposite direction with a mean negative velocity

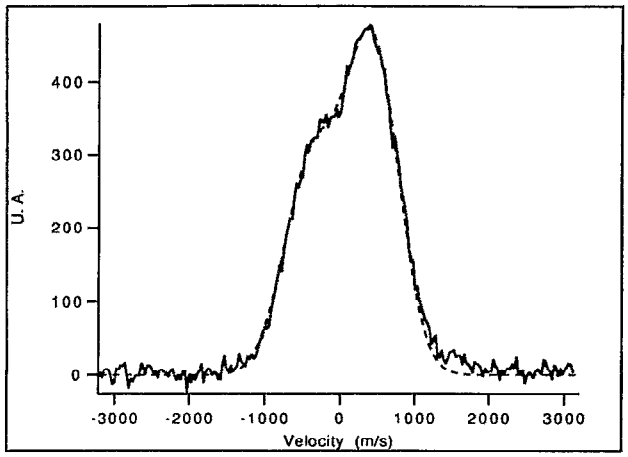

(a)

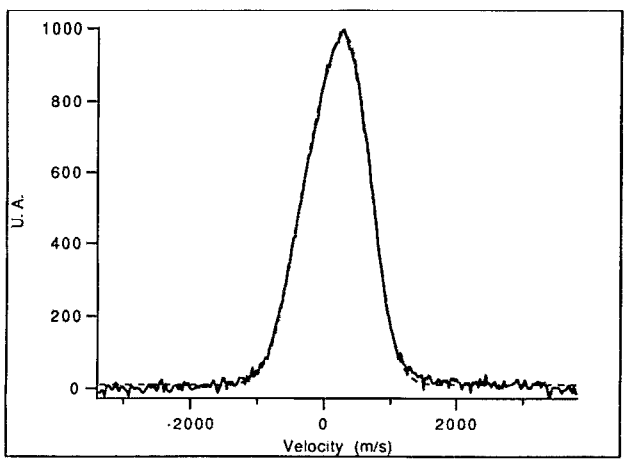

(b)

FIG. 4. Longitudinal velocity distribution function for two measurement positions: (a) near the door and (b) at the center of the device.

equal to -0.36 km/sec. The dashed curve of Fig. 4(a) is obtained by fitting the continuous curve by two drifting Maxwellian curves that have different amplitudes but the same temperature, equal to 0.05 eV.

The continuous curve of Fig. 4(b) shows a measurement of the longitudinal ion velocity distribution near the center of the device. At first glance a single hump is observed. But the temperature determined using a one-Gaussian model is higher than our previous experimental results by a factor 2.5. A more careful inspection shows that the peak velocity is slightly shifted above zero. So it seems that there are, in fact, two Gaussians too close together to be resolved. By fitting a two-Gaussian model, the same ion temperature is obtained as near the door, as shown by the dashed curve on Fig. 4(b).

These results can be interpreted in terms of (i) an ion drift due to the longitudinal plasma density gradient and associated potential drop combined with (ii) a nonelastic reflection on the multipolar magnetic field at the far end of the machine. The model we used by considering drifting Maxwellian curves is probably not fully justified, as we will see in the next part, but it is sufficient to illustrate the fact

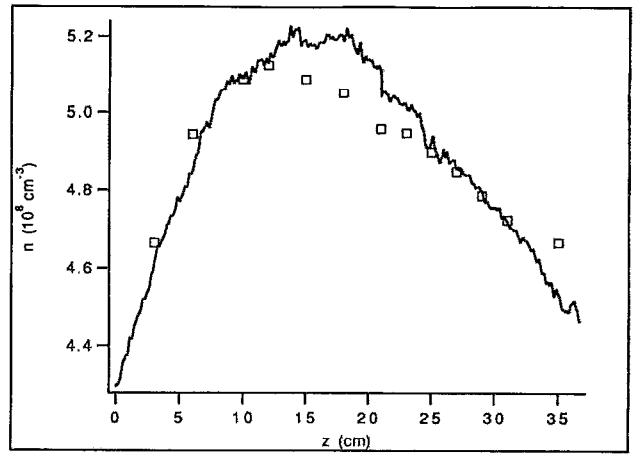

FIG. 5. ——, axial plasma density profile measured by a movable Langmuir probe. □, density from local plasma potential calculated from the measured mean velocity. The filament holder is at $z=0$ cm.

that great care must be taken in the determination of the ion temperature.

C. Non-Maxwellian components for the ion distribution function

In the previous paragraph, we have interpreted the largest observed ion drift as the effect of the plasma density gradient. In order to confirm this result, the four rows of permanent magnets have been removed from the end door, which is closer to the filament holder No. 1. The rows of permanent magnets are kept on the opposite end door closer to the filament holder No. 2. The argon working pressure is equal to 6.4×10^{-4} Torr, and the discharge voltage and current are, respectively, equal to 50 V and 1 A.

When filament holder No. 2 is used to create the plasma, the position of the maximum density profile is shifted toward the end door, bearing the permanent magnet rows, and roughly corresponds to the filament holder position. On the side of the unmagnetized door where the possibility of ion reflection on the multipolar magnetic field has been suppressed, the measured longitudinal ion distribution function exhibits a single hump, as expected. The mean velocity of the hump increases as the measurement is made closer and closer to the unmagnetized door, because the drop in the plasma potential causes the ions to become accelerated. On the side of the magnetized door, there is a double hump distribution function, as observed on Fig. 4. This clearly demonstrates the influence of the multipolar magnetic field on ion reflection.

When filament holder No. 1 bearing four filaments inside the magnetic cusps is used to create the plasma, the resulting plasma density profile along the axis of the device is shown in Fig. 5. It is obtained by plotting the electron saturation current as a function of the axial position of a movable plane Langmuir probe. The spatial origin corresponds to the position of the copper ring of the filament holder situated closer to the plasma. The maximum density

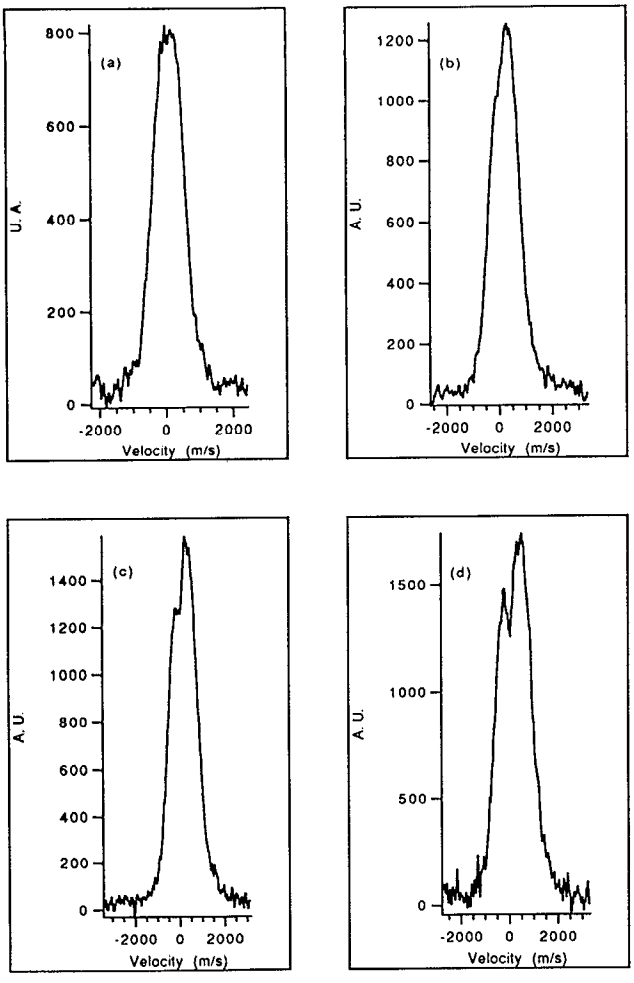

FIG. 6. Evolution of the longitudinal velocity distribution function: (a) at $z=15$ cm, (b) at $z=24$ cm, (c) at $z=28$ cm, and (d) at $z=31$ cm. The filament holder is at $z=0$ cm and the magnetized end door is at $z=55$ cm.

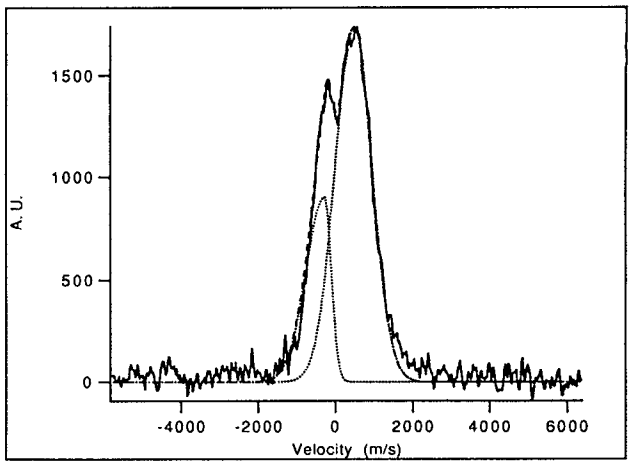

FIG. 7. Reconstruction of the longitudinal ion velocity distribution function of Fig. 6(d).

profile corresponds to the center of the device. As expected, the density profile is asymmetrical, with a larger density gradient on the side where the magnet rows are missing. Note that Fig. 5 gives a closeup view of the density profile near its maximum. The origin of the vertical axis is not shown.

Figure 6 shows the longitudinal ion distribution function measured at four different positions. As we are exploring the region located between the filament holder and the magnetized door, we find a double hump distribution function characteristic of ion reflection on the multipolar magnetic field, as before. Closer to the filaments, Fig. 6(a) shows a strong overlapping of the two drifting components, while these two components can be easily resolved on Fig. 6(d) closer to the end door.

Several attempts to fit the double humped distributions of Fig. 6 have been made. It is *not* possible to reproduce the double hump, using only the superposition of two Maxwellian curves characterized by five parameters (four parameters for the amplitude and the mean drift velocity of each component, and one parameter for the common ion temperature) as we did previously for Fig. 4, where the two components were not clearly resolved.

One empirical way to reconstruct the observed distribution is displayed in Fig. 7, where the continuous curve corresponds to the measured curve of Fig. 6(d). The dashed curve of Fig. 7 corresponds to the superposition of the two dotted components, and gives a fairly good representation of the experimental curve. The large dotted component with positive mean velocity is a drifting Maxwellian curve with a temperature equal to 0.07 eV and corresponds to an ion population accelerated toward the magnetized end door. The small, dotted component, corresponding to the reflected ion population, is made of two halves: the left half is a half-Maxwellian curve with a temperature equal to 0.07 eV as before and the right half is another half-Maxwellian curve with a lower temperature equal to 0.02 eV. The physical meaning of this representation is that some reflected ions do not have a longitudinal velocity large enough to climb the potential gradient. This explanation is consistent with analytic calculations.[13] A still more accurate description should take into account the modification of the Maxwellian distribution by the ion acceleration. But for the rather moderate observed density variations, this modification is not very significant.

From the measured mean velocity, we can deduce the local plasma potential $\Phi(x)$ that can lead to such an ion acceleration when the ions are at rest at x_m and $\Phi(x_m)=0$, where x_m is the position of the density maximum. Assuming that the electrons in the discharge have a Boltzmannian behavior with a measured temperature of kT_e, the relative density gradient can be related to the normalized local potential $e\Phi(x)/kT_e$. Reporting the result of such a calculation at various positions, we obtain the points of Fig. 5, which are in close accordance with the measured density profile.

V. CONCLUSIONS

We used a laser-induced fluorescence diagnostic to study the ion behavior of an argon plasma discharge in a

multipolar device. Several configurations have been studied; they all show the impressive potential of this diagnostic.

We have been able to show the spatial localization of ionization processes when the filaments emitting primary electrons are inside the multipolar magnetic field.

The ion acceleration in very weak density gradients can be accurately measured. Ion distribution functions exhibiting double humps have been measured and explained by ion reflection on the multipolar magnetic field. In many cases, the two humps can overlap so closely that they are almost indistinguishable. This fact must be taken into account in the precise determination of the ion temperature. Moreover, the observation of the modification of a Maxwellian distribution due to acceleration and reflection of the ions has been made possible by this powerful technique.

The observed superposition of drifting ion populations may be responsible for the low-frequency noise currently reported in multipolar devices.

ACKNOWLEDGMENTS

We wish to thank P. Louvet and R. A. Stern for stimulating conversations. The technical assistance of J. C. Chezeaux and B. Squizzaro is greatly appreciated.

L. C. and M. C. are supported by grants from the Ministère de la Recherche et de la Technologie.

[1]R. Measures, J. Appl. Phys. **39**, 5232 (1968).
[2]R. A. Stern and J. A. Johnson, Phys. Rev. Lett. **34**, 1548 (1975).
[3]D. N. Hill, S. Fornaca, and M. G. Wickham, Rev. Sci. Instrum. **54**, 309 (1983).
[4]R. A. Stern, D. N. Hill, and N. Rynn, Phys. Rev. Lett. **47**, 792 (1981).
[5]F. Anderregg, Ph.D. thesis, Ecole Polytechnique Fédérale de Lausanne, Lausanne, Switzerland, 1989.
[6]M. J. Goeckner, J. Goree, and T. E. Sheridan, Phys. Fluids B **3**, 2913 (1991).
[7]R. Limpaecher and K. R. MacKenzie, Rev. Sci. Instrum. **44**, 726 (1973).
[8]H. Ikesi and R. J. Taylor, Phys. Rev. Lett. **22**, 923 (1969).
[9]D. Grésillon, J. Phys. **32**, 269 (1971).
[10]J. L. Cooney, M. T. Gavin, J. E. Williams, D. W. Aossey, and K. E. Lonngren, Phys. Fluids B **3**, 3277 (1991).
[11]J. Perrin and G. W. Hamilton, Chem. Phys. **67**, 167 (1982).
[12]C. Gauthereau and G. Matthieussent, Phys. Lett. A **102**, 231 (1984).
[13]G. A. Emmert, R. M. Wieland, T. Mense, and J. N. Davidson, Phys. Fluids **23**, 803 (1980).
[14]W. Gekelman, R. L. Stenzel, and N. Wild, J. Geophys. Res. **87**, 101 (1982).